Thermodynamic Analysis of the Temperature Dependence of OH Adsorption on Pt(111) and Pt(100) Electrodes in Acidic Media in the Absence of Specific Anion Adsorption

Víctor Climent, Roberto Gómez, José M. Orts,* and Juan M. Feliu

Departamento de Química Física e Instituto Universitario de Electroquímica, Universidad de Alicante, Apartado 99, E−03080 Alicante, Spain

Received: September 1, 2005; In Final Form: April 4, 2006

The effect of temperature on the voltammetric OH adsorption on Pt(111) and Pt(100) electrodes in perchloric acid media has been studied. From a thermodynamic analysis based on a generalized adsorption isotherm, $\Delta G°$, $\Delta H°$, and $\Delta S°$ values for the adsorption of OH have been determined. On Pt(111), the adsorption enthalpy ranges between −265 and −235 kJ mol^{-1}, becoming less exothermic as the OH coverage increases. These values are in reasonable agreement with experimental data and calculated values for the same reaction in gas phase. The adsorption entropy for OH adsorption on Pt(111) ranges from −200 J mol^{-1} K^{-1} (low coverage) to −110 J mol^{-1} K^{-1} (high coverage). On the other hand, the enthalpy and entropy of hydroxyl adsorption on Pt(100) are less sensitive to coverage variations, with values ca. $\Delta H° = -280$ kJ mol^{-1} and $\Delta S° = -180$ J mol^{-1} K^{-1}. The different dependence of $\Delta S°$ with coverage on both electrode surfaces stresses the important effect of the substrate symmetry on the mobility of adsorbed OH species within the water network directly attached to the metal surface.

1. Introduction

The adsorption of OH species on metal surfaces is undoubtedly a process of paramount importance in surface electrochemistry, in particular, for noble metals such as platinum. From an electrocatalytic point of view, adsorbed hydroxyl, OH_{ads}, is a key intermediate in the electrooxidation of many compounds, the best known example probably being the oxidation of carbon monoxide adsorbed on platinum electrodes.[1−6] This reaction has been studied on a number of well-defined platinum single-crystal surfaces with different crystallographic orientations and for different electrolytes.

In the absence of chemisorption of the electrolyte anions, the formation of OH_{ads} on Pt(111) and Pt(100) takes place in wide potential regions positive to the potential of zero charge (PZC) of these surfaces but significantly less positive than the threshold for the formation of the surface oxide phases. The reversibility of the voltammograms in the potential region where OH adsorption/desorption occurs makes possible the study of the Pt−OH system by means of an equilibrium thermodynamic analysis of the temperature dependence of the voltammetric features for this process. This approach, initially used by Breiter[7] and Conway[8] with polycrystalline platinum electrodes, has been applied by different groups[9−14] to the study of adsorption processes on platinum single-crystal electrodes. The method allows one to calculate the standard changes of enthalphy and entropy for an overall reaction including the processes taking place at the reference electrode. Also, the effective lateral interaction parameter and the adsorbate binding energy to the surface can be estimated.

In a recent paper,[14] we have shown from a temperature-dependence analysis that the values of entropy changes corresponding to the formation of H_{ads} on Pt(111), Pt(100), and Pt(110) electrodes in perchloric acid medium indicate significant changes in the degree of order of the adsorbed water layer upon hydrogen adsorption. These can be rationalized as a consequence of the mismatch between the metal surface structure and that of water at the interface.

The study of the formation of OH adlayers in the metal/aqueous electrolyte interface has additional interest and difficulties. First of all, theoretical calculations indicate that, on the most studied Pt(111) surface, both water[15] and OH[16,17] adsorb at on-top positions. This means that their adsorption is competitive. Additionally, in acidic medium, OH_{ads} is not expected to be formed from aqueous (or adsorbed) OH^- anion, but probably from an adsorbed water molecule which competes for the same on-top adsorption sites. Moreover, the ability of both species to form hydrogen bonds allows for the formation of extended water−OH networks in the surface layer.[18] Recently, the structures of OH adlayers and water−OH coadsorbed layers have been studied both experimentally (under UHV conditions)[19−21] and theoretically.[22,23]

In this paper, the dependence of the voltammetric behavior of platinum single-crystal electrodes with (111) and (100) orientations is studied in the potential region between the PZC and 0.90 V RHE (reversible hydrogen electrode). In the case of Pt(111), this corresponds to the once controversial "butterfly" features first reported by Clavilier.[24] A previous experimental study exists for Pt(111) by Markovic et al.,[13] but with a data interpretation different from that contained in this paper. The aim of this paper is to present a new thermodynamic analysis for the hydroxyl adsorption process on metal electrodes and then to apply it to the case of platinum single-crystal surfaces.

2. Experimental Section

Platinum single-crystal electrodes were prepared according to the procedure described in ref 25. Before each experiment, the electrode was annealed in a gas + air flame and cooled in a hydrogen + argon atmosphere.[26] Afterward, the electrode

* Corresponding author. jm.orts@ua.es.

10.1021/jp054948x CCC: $33.50
Published on Web 05/20/2006

surface was protected with a droplet of ultrapure water saturated with these gases and transferred to the electrochemical cell.

A two-compartment, all-Pyrex electrochemical cell was used. The electrochemical cell was immersed in a water bath whose temperature was controlled within ±0.1 K by a thermostat (Haake FK). The temperature in the water bath was measured with a platinum resistance thermometer (±0.1 K, Crison 638Pt). The experiments were carried out at six temperatures between 273 and 323 K at intervals of 10 K. All potentials were measured against a reversible hydrogen electrode, RHE, immersed in the same working solution and at the same temperature as the working electrode (the so-called isothermal configuration). A coiled Pt wire was used as a counter electrode.

Aqueous solutions were prepared from concentrated $HClO_4$ (Merck Suprapur) and ultrapure water from a Millipore system (MilliQ plus 185).

The electrochemical instrumentation consisted of an EG&G PAR Model 175 universal programmer, an AMEL 551 potentiostat, and a Philips PM 8133 X−Y recorder.

3. Results and Discussion

3.1. Thermodynamic Treatment for OH Adsorption in Acidic Media, in the Absence of Specific Adsorption. As stated in the Introduction, the voltammetric currents corresponding to hydrogen adsorption and their temperature dependence have been previously analyzed[14] by applying a thermodynamic analysis based on the use of a generalized adsorption isotherm. This isotherm has previously been used to analyze electrochemical adsorption data by Blomgren and Bockris,[27] by Ross,[28] and by Jerkiewicz and Zolfaghari.[29] In the following, we apply essentially the same analysis to the OH adsorption region.

In the OH adsorption region, the following reaction takes place at the working electrode

$$H_2O + Pt \rightleftharpoons Pt{-}OH + H^+ + e^W \qquad (1)$$

which together with the reaction at the reference electrode

$$H^+ + e^R \rightleftharpoons 1/2H_2 \qquad (2)$$

gives the overall reaction

$$H_2O + Pt + e^R \rightleftharpoons Pt{-}OH + 1/2H_2 + e^W \qquad (3)$$

where e^W and e^R stand for the electrons in the working and reference electrodes, respectively. The equilibrium condition for reaction 3 is

$$\mu_{OH,a} + {}^1/_2\mu_{H_2} - \mu_{H_2O} + \bar{\mu}_e{}^W - \bar{\mu}_e{}^R = 0 \qquad (4)$$

where μ_i stands for the chemical potential of species i, and $\bar{\mu}_e{}^W$ and $\bar{\mu}_e{}^R$ stand for the electrochemical potential of electrons, in the working and in the reference electrode, respectively. The difference between both electrochemical potentials is related to the measured cell potential (E), which can thus be used for calculating the chemical contribution to the change in the Gibbs energy involved in reaction 3

$$FE = \Delta G = \mu_{OH,a} + {}^1/_2\mu_{H_2} - \mu_{H_2O} \qquad (5)$$

The chemical potentials of H_2 and H_2O can be considered equal to those of the pure substances, $\mu^0_{H_2}$ and $\mu^0_{H_2O}$, respectively (i.e., $f_{H_2} \approx 1$ bar and $a_{H_2O} \approx 1$), while the dependence of the chemical potential of the adsorbed OH with temperature and coverage can be taken as

$$\mu_{OH,a} = \mu^0_{OH,a} + RT\ln\left(\frac{\theta_{OH}}{1-\theta_{OH}}\right) + r(\theta_{OH}) \qquad (6)$$

where the term $r(\theta_{OH})$ includes all the deviations from the ideal Langmuirian behavior. In the case of the Frumkin isotherm, this term would be $r(\theta_{OH}) = \omega\theta_{OH}$ where ω is a constant (Frumkin lateral interaction parameter). Following the methodology of refs 14 and 30 and the arguments by Conway et al.,[31] it is convenient to define a formal standard Gibbs energy for reaction 3 that includes the $r(\theta)$ term, according to

$$\Delta G°(\theta_{OH}) = \mu^0_{OH,a} + {}^1/_2\mu^0_{H_2} - \mu^0_{H_2O} + r(\theta_{OH}) \qquad (7)$$

The reader should note that, since such a formal standard energy is coverage-dependent, it is not a true standard energy.

With this definition, eq 5 becomes

$$FE = \Delta G°(\theta_{OH}) + RT\ln\left(\frac{\theta_{OH}}{1-\theta_{OH}}\right) \qquad (8)$$

which can be written as a generalized adsorption isotherm[27]

$$\frac{\theta_{OH}}{1-\theta_{OH}} = \exp\left(-\frac{\Delta G°(\theta_{OH})}{RT}\right)\cdot\exp\left(\frac{F}{RT}E\right) \qquad (9)$$

The latter equation will be the basis of the thermodynamic analysis given below.

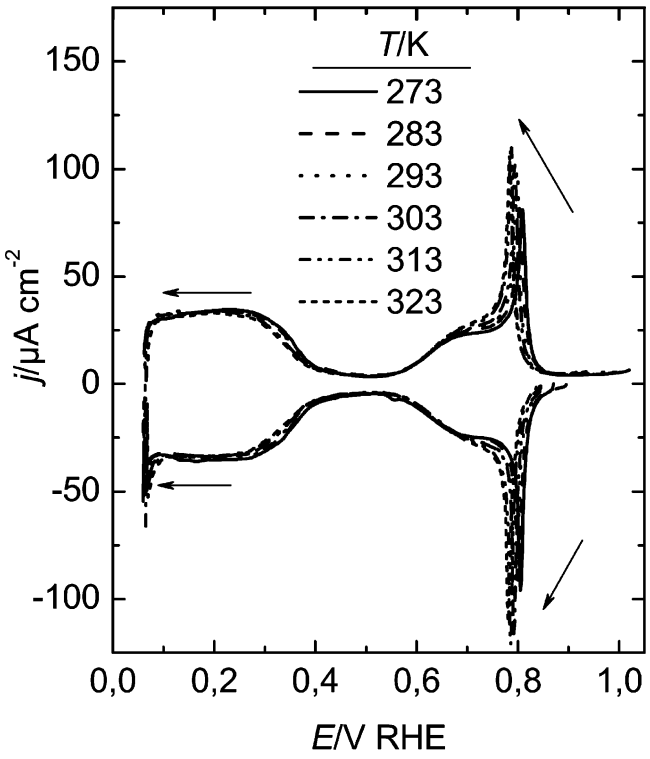

Figure 1. Cyclic voltammograms corresponding to a Pt(111) electrode in a 0.1 M $HClO_4$ solution at different temperatures. Scan rate: 50 mV s^{-1}. Arrows indicate the direction of the changes associated with an increase of temperature.

3.2. OH Adsorption on Pt(111) Electrodes in 0.1 M Perchloric Acid Solution. Figure 1 shows six cyclic voltammograms obtained for a Pt(111) electrode in a 0.1 M $HClO_4$ solution at different temperatures, ranging from 273 to 323 K.

These voltammograms show all the well-established features corresponding to hydrogen and OH adsorption phenomena on a clean, well-ordered Pt(111) surface. Hydrogen adsorption[14] takes place at potentials lower than 0.4 V, while OH adsorption occurs at potentials above 0.55 V. The absence of distinguishable peaks in the hydrogen adsorption region attests the virtual absence of (110) or (100) defects on the surface. The height and sharpness of the spike at 0.80 V are also indications of both the quality of the surface and the cleanliness of the solution. An increase of the working temperature does not significantly change the shape of the voltammogram, but shifts both the hydrogen and OH adsorption regions to lower potential values in the RHE scale. The charge density integrated under the hydrogen and hydroxyl adsorption regions remains also essentially unchanged. All these results agree well with previously published work.[13,14]

The first step in the calculation of the formal standard Gibbs energy, $\Delta G°(\theta_{OH})$, through eq 8, is to subtract the Langmuirian configurational term, $RT \ln(\theta_{OH}/(1 - \theta_{OH}))$, from the Gibbs energy change, FE. The OH coverage can be calculated by integrating the voltammetric current density above 0.55 V, according to

$$\theta_{OH}(E) = \frac{1}{q_{ML}} \int_{0.55}^{E} \frac{j - j_{dl}}{\upsilon} \mathrm{d}E \qquad (10)$$

where υ is the sweep rate (50 mV s^{-1} for the voltammograms of Figure 1), q_{ML} is the charge density corresponding to the formation of a saturated OH adlayer, and j_{dl} is the current density contribution corresponding to the charging of the double layer. To minimize any errors that could arise in the integration because of the existence of small negative currents due to the reduction of oxygen traces, the voltammetric current was taken as the average of the positive- and negative-going sweeps. The value of q_{ML} can be obtained from the maximum charge integrated from the voltammogram, assuming that the maximum OH coverage is attained at the higher potential limit, past the spike. This gives a value for q_{ML} of 109 ± 3 μC cm^{-2}, with no significant dependence on the temperature. This value of q_{ML} corresponds to ca. 0.45 ± 0.01 OH species per surface platinum atom. It should be noted, however, that the OH coverage values obtained from eq 10 are directly normalized to 1, as required by eqs 6−9. On the other hand, the double-layer contribution is assumed to be constant and equal to the value of the current in the double-layer region around 0.5 V, which is the same value observed at higher potentials (0.9 V). This value, 4.0 ± 0.2 μA cm^{-2} does not vary significantly with temperature.

Figure 2 shows the integration of the voltammograms for the different temperatures. The resulting normalized coverage values can be inserted into eq 8 to calculate the formal standard Gibbs energy of reaction 3, shown in Figure 3A. Due to the term $\ln(\theta_{OH}/(1 - \theta_{OH}))$, the uncertainty in the calculation is larger when either $\theta \rightarrow 0$ or $\theta \rightarrow 1$. For $0.1 < \theta < 0.5$, $\Delta G°(\theta_{OH})$ varies almost linearly with the coverage, suggesting that the Frumkin isotherm is valid in this coverage range,[32] and $\Delta G°(\theta_{OH})$ can be represented by the following expression:

$$\Delta G°(\theta_{OH}) = \Delta G°(\theta_{OH} \rightarrow 0) + \omega\theta_{OH} \qquad (11)$$

where ω is the lateral interaction parameter. The quantity $\Delta G°(\theta_{OH} \rightarrow 0)$ can be considered as a true standard value, as long as in the zero coverage limit, $r(\theta_{OH}) = 0$ (see eq 7).

The slope decreases when the temperature is increased. This indicates a decrease in the lateral interaction parameter (that contains enthalpic as well as entropic contributions to the Gibbs energy) with the increase of temperature. All the curves cross one another around the same coverage value, $\theta_{OH} \approx 0.35$. At

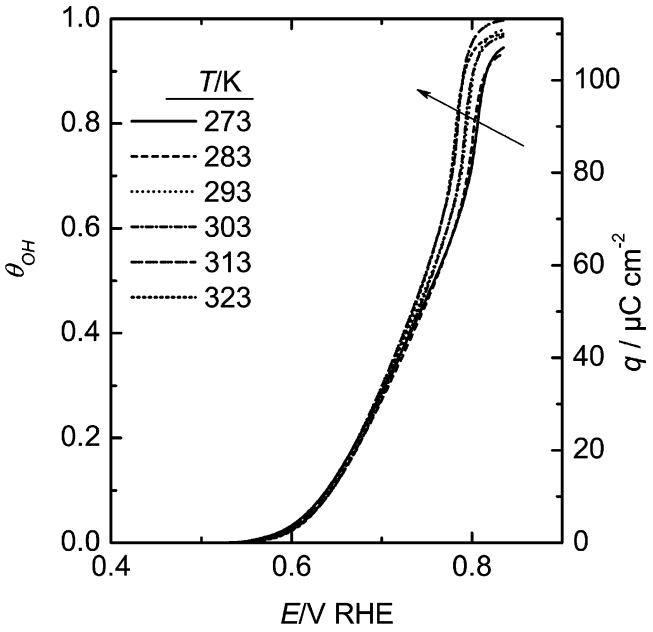

Figure 2. Charge density of OH adsorption and normalized OH coverage obtained by integration of the voltammograms of Figure 1. The arrow indicates the direction of the change associated with the increase of temperature.

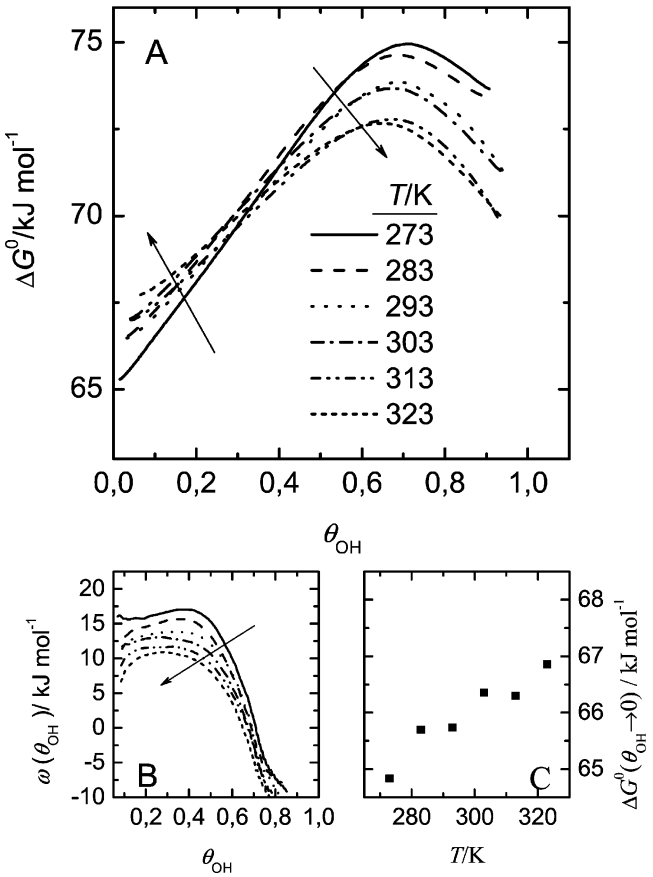

Figure 3. (A) Plot of $\Delta G°$ for the process $H_2O + Pt(111) \rightleftharpoons Pt(111)-OH + {}^1/_2H_2$ as a function of OH coverage for different temperatures. (B) Plot of the lateral interaction parameter, $\omega(\theta_{OH}) = (\partial \Delta G°/\partial \theta_{OH})_T$, as a function of OH coverage. (C) Extrapolated values of $\Delta G°$ to zero coverage as a function of the temperature. Arrows in A and B indicate the increase of temperature.

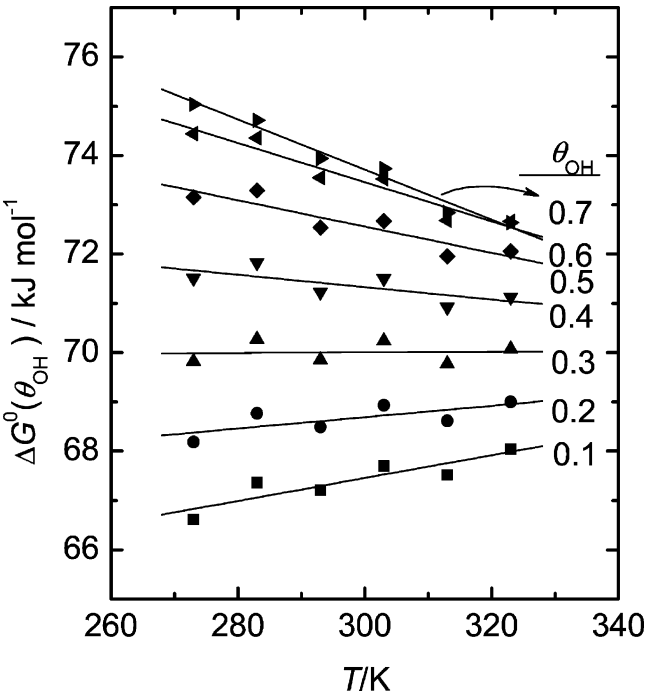

Figure 4. Plot of $\Delta G°$ for the process H_2O + Pt(111) ⇋ Pt(111)−OH + $^1/_2H_2$ as a function of the temperature for different values of OH coverage. Lines are best fits to experimental data.

this particular coverage, $\Delta G°$ is nearly independent of the temperature (see below).

The lateral interaction parameter can be obtained as the following partial derivative:

$$\omega(\theta_{OH}, T) = \left[\frac{\partial \Delta G(\theta_{OH})}{\partial \theta_{OH}}\right]_T \qquad (12)$$

The result of differentiating the curves of Figure 3A is shown in Figure 3B. As anticipated above, the interaction parameter is nearly constant in the range $0.1 < \theta_{OH} < 0.5$. Typical values range between 10 and 15 kJ mol^{-1} (on the order of a typical hydrogen bond), while a marked decrease takes place at coverage above 0.5, becoming negative (attractive interactions) at coverage values higher than 0.6 (around 0.3 OH/Pt). This corresponds to the region of the spike.

The region where the dependence of $\Delta G°$ with coverage is linear can be used to determine the standard Gibbs energy for reaction 3 in the limit of zero coverage. The values for this quantity for the different temperatures studied are around 66 kJ mol^{-1} (shown in Figure 3C). An almost linear increase of $\Delta G°(\theta_{OH} \rightarrow 0)$ with the temperature can be observed in this plot. The increase, however, is small (around 40 J mol^{-1} K^{-1}).

The entropy change associated with reaction 3 can be calculated by evaluating the following partial derivative:

$$\Delta S°(\theta_{OH}) = -\left(\frac{\partial \Delta G°}{\partial T}\right)_{\theta_{OH}} \qquad (13)$$

To evaluate this derivative, we have plotted the values of $\Delta G°(\theta)$ as a function of temperature for different values of coverage (seven of these curves are shown in Figure 4). The resulting plots are nearly linear. As anticipated above, the slope of the lines changes from positive to negative when the coverage attains a value of 0.35. The resulting curves have been fitted to straight lines, and their slopes have been used to calculate the entropy change of the adsorption reaction, according to eq 13.

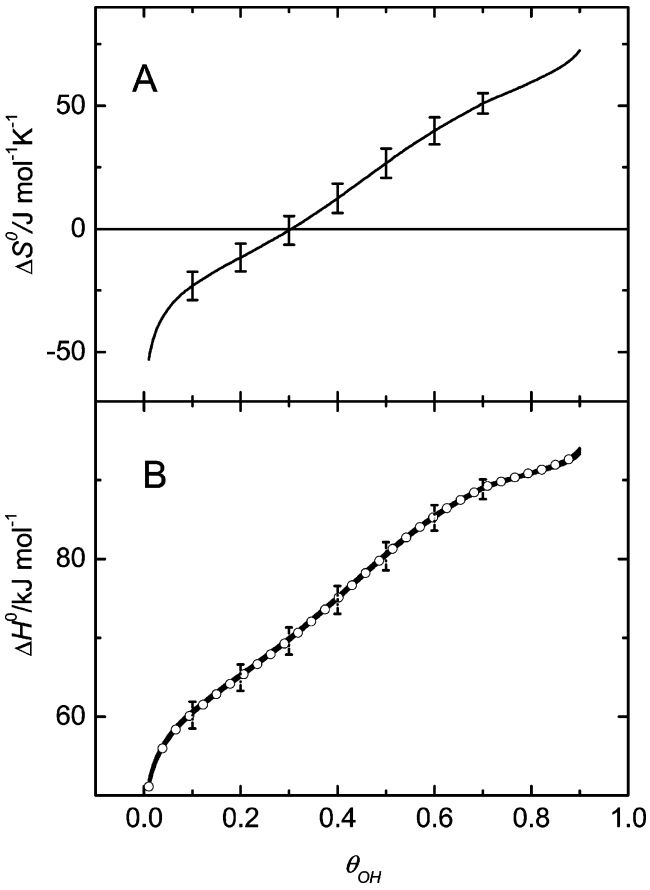

Figure 5. Plots of (A) $\Delta S°$ and (B) $\Delta H°$ for the process H_2O + Pt(111) ⇋ Pt(111)−OH + $^1/_2H_2$ as a function of OH coverage, as calculated from the slopes of the plots of Figure 4. Error bars are calculated from the uncertainty resulting from the linear regression. Circles in (B) correspond to values determined with the Gibbs−Helmholtz equation.

The entropy values are plotted in Figure 5A as a function of OH coverage. Since a linear fit has been used to determine the partial derivative of eq 13, a single curve $\Delta S°$ vs θ_{OH} is obtained, independent of temperature. Error bars in this figure reflect the uncertainty associated to the least-squares regression. The value of $\Delta S°$ at low coverage approximately agrees with the value obtained from the slope of the $\Delta G°(\theta_{OH} \rightarrow 0)$ vs T plot. $\Delta S°$ $(\theta_{OH} \rightarrow 0)$ attains a value of −40 J mol^{-1}K^{-1} and can be considered as a true standard value.

Finally, the coverage-dependent formal standard enthalpy for reaction 3 can be calculated as

$$\Delta H°(\theta) = \Delta G°(\theta) + T\Delta S°(\theta) \qquad (14)$$

Again, since $\Delta G°(\theta_{OH})$ has been assumed to depend linearly on temperature, a single, temperature-independent curve is obtained for $\Delta H°(\theta_{OH})$. The result is shown in Figure 5B. The standard value $\Delta H°(\theta_{OH} \rightarrow 0)$ can be calculated directly from eq 14 once the values for $\Delta S°(\theta_{OH} \rightarrow 0)$ and $\Delta G°(\theta_{OH} \rightarrow 0)$ are known. The resulting value is 54.5 kJ mol^{-1}, in agreement with the values of $\Delta H°$ for low θ_{OH} in Figure 5B.

Alternatively, $\Delta H°$ can be calculated with the Gibbs−Helmholtz equation

$$\Delta H°(\theta_{OH}) = F\left(\frac{\partial E/T}{\partial 1/T}\right)_{\theta_{OH}} \qquad (15)$$

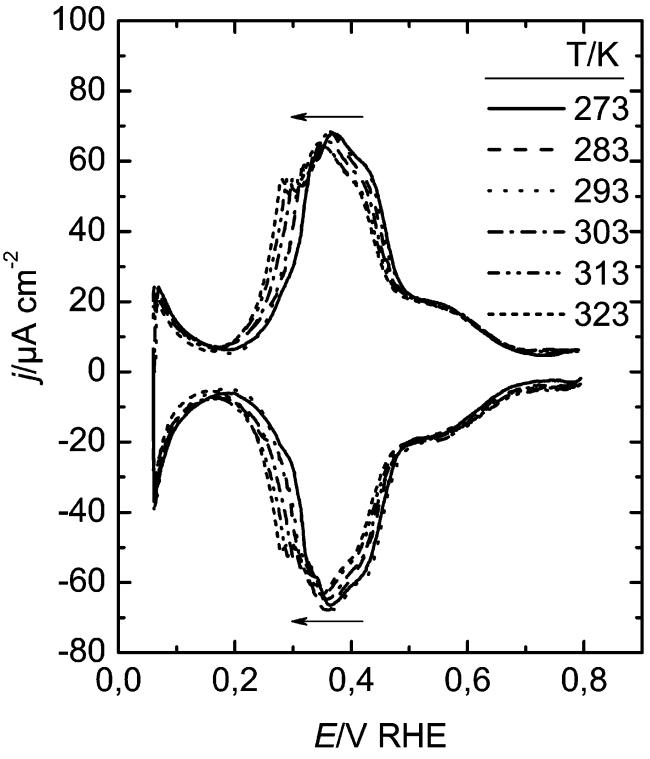

Figure 6. Cyclic voltammograms corresponding to a Pt(100) electrode in a 0.1 M $HClO_4$ solution at different temperatures. Scan rate: 50 mV s^{-1}. Arrows indicate the direction of the changes associated with an increase of the temperature.

This alternative method for calculating $\Delta H°$ gives identical results, as can be seen in Figure 5B. Values of the enthalpy change associated to reaction 3 range between 50 and 100 kJ mol^{-1}.

3.3. OH Adsorption on Pt(100) Electrodes in 0.1 M Perchloric Acid Solution. Figure 6 shows cyclic voltammograms corresponding to the Pt(100) surface in 0.1 M perchloric acid at different temperatures. The voltammograms show the characteristic adsorption states corresponding to a well-ordered Pt(100) electrode surface. The broad peak centered at ca. 0.36 V corresponds to hydrogen adsorption on wide two-dimensional (100) domains, while the shoulder located between 0.5 and 0.75 V corresponds to OH adsorption. As with Pt(111), a temperature increase results in a significant displacement of the hydrogen adsorption states toward lower potentials, without a noticeable decrease in their associated charge density. On the other hand, the position of the OH adsorption states is less sensitive to the temperature of the working solution.

A problem that arises when applying the previous thermodynamic analysis to the OH adsorption on Pt(100) electrodes is the significant overlapping existing between the hydrogen and the OH adsorption regions.[14] This overlapping precludes the direct determination of the maximum OH coverage from the integration of the voltammetric current density. As explained in ref 14, the hydrogen and OH contributions can be separated by taking into account the results of charge displacement experiments. With this method, a maximum value of 0.37 OH species per surface platinum atom is obtained, nearly independent of temperature within the accuracy of the experimental technique. With this information, the dependence of θ_{OH} on the electrode potential can be obtained by integrating the voltammetric currents from 0.75 V backward, down to ca. 0.5 V, where hydrogen adsorption begins. Once the normalized OH coverage is calculated, application of eq 8 allows the determination of the Gibbs energy associated with reaction 3 on Pt(100). The

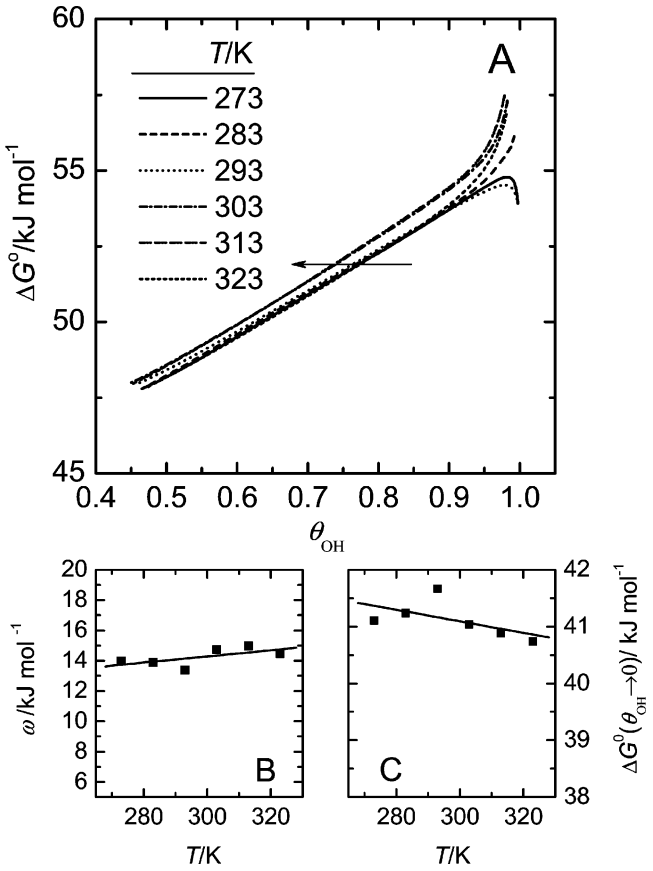

Figure 7. (A) Plot of $\Delta G°$ for the process $H_2O + Pt(100) \rightleftharpoons Pt(100)-OH + {}^1/_2H_2$ as a function of OH coverage for different temperatures. (B) Extrapolated values of $\Delta G°$ to zero coverage as a function of temperature. (C) Plot of the lateral interaction parameter, $\omega = d\Delta G°/d\theta_{OH}$, as a function of temperature. Straight lines in B and C are best fits to the experimental points. The arrow in A indicates the evolution for increasing temperatures.

results are shown in Figure 7A. The plot of $\Delta G°$ versus θ_{OH} gives nearly straight lines, allowing the use of linear regression to obtain the extrapolated value of $\Delta G°$ at zero coverage, $\Delta G°(\theta_{OH} \rightarrow 0)$, and the Frumkin lateral interaction parameter, ω. As opposed to the case of Pt(111), nearly parallel lines are obtained for Pt(100). This indicates that the lateral interaction parameter is nearly independent of temperature for this electrode. The linearity of the plot allows extrapolation of $\Delta G°$ to θ_{OH} values lower than 0.5, in the hydrogen adsorption region. This approach is equivalent to fitting the OH adsorption region to a Frumkin isotherm and has been used in the past to separate hydrogen and OH adsorption contributions to the voltammetric current.[14,30] The effect of temperature on the lateral interaction parameter, ω, and on $\Delta G°(\theta_{OH} \rightarrow 0)$ is shown in Figure 7B and C, respectively. The values for the former scatter around 14 kJ mol^{-1}. This value agrees well with those measured for Pt(111) in the low-coverage range (Figure 3B). However, as anticipated above, this parameter is not so sensitive to temperature variation. On the other hand, the values of $\Delta G°(\theta_{OH} \rightarrow 0)$ for Pt(100) are significantly lower than for Pt(111).

Figure 8 shows the resulting values of $\Delta S°$ and $\Delta H°$ obtained from eqs 13 and 14. The values at $\theta_{OH} < 0.5$ result from the linear extrapolation of $\Delta G°$. Values of $\Delta S°$ are very close to zero, within the experimental uncertainty, and change little with coverage. This is directly related to the small dependence of the OH voltammetric adsorption with temperature and is significantly different from the result obtained for Pt(111). The

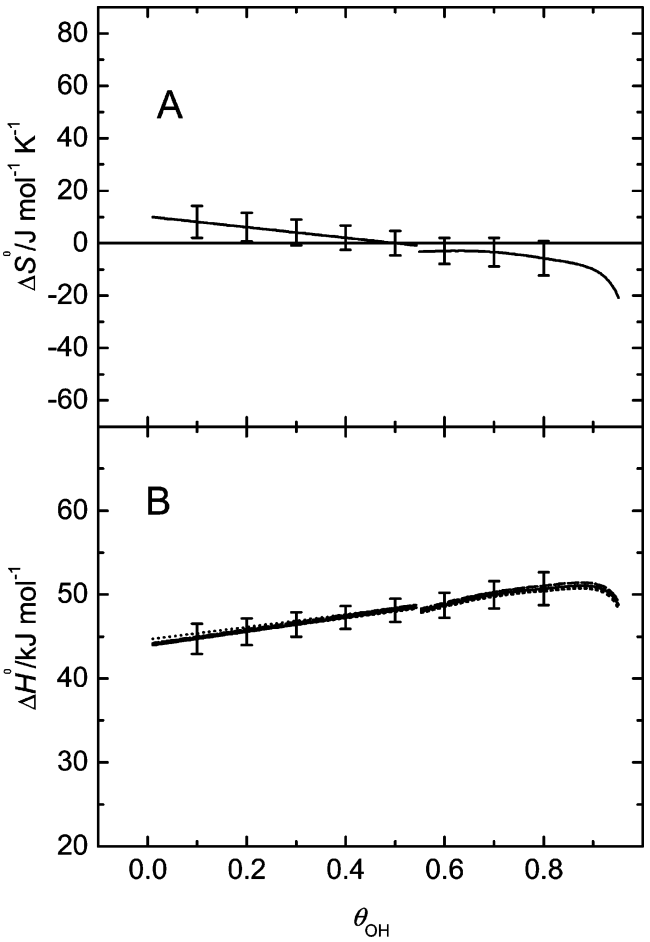

Figure 8. Plots of (A) $\Delta S°$ and (B) $\Delta H°$ for the process H_2O + Pt(100) ⇌ Pt(100)−OH + $^1/_2H_2$ as a function of OH coverage. Values at $\theta_{OH} < 0.55$ are calculated from a linear extrapolation of $\Delta G°$ values in Figure 7A. Error bars are calculated from the uncertainty resulting from the linear regression.

TABLE 1: Thermodynamic Parameters for Liquid Water Formation from Gas-Phase Hydroxyl Radical and Molecular Hydrogen at 298 K

reaction	$\Delta G°$ kJ mol^{-1}	$\Delta H°$ kJ mol^{-1}	$\Delta S°$ J mol^{-1} K^{-1}
$OH(g) + {}^1/_2H_2(g) \rightleftharpoons H_2O(l)$	−271	−325	−179

values of $\Delta H°$ are located around 45 kJ mol^{-1} and also exhibit less dependence with the coverage than in the case of Pt(111).

3.4. Discussion of Results and Comparison with Literature Data. One drawback of the previous thermodynamic analysis is that all the determined thermodynamic functions correspond to reaction 3. These results are not easy to interpret in a direct way, since this reaction involves not only the formation of a platinum−OH bond but also the splitting of a water molecule and the formation of a H−H bond. A more straightforward analysis can be carried out if the results previously shown are combined with the known standard potential and thermal coefficient for the reaction of formation of a hydroxyl radical[33]

$$OH(g) + H^+(aq) + e \rightleftharpoons H_2O(l) \quad E° = 2.813\ V \qquad (d E°/dT) = -1.856\ mV\ K^{-1} \quad (16)$$

Resulting values of $\Delta G°$, $\Delta H°$, and $\Delta S°$ for this reaction at 298 K are summarized in Table 1 (calculated by taking into account that $E° = 0.0000$ V for $H^+(aq) + e \rightleftharpoons {}^1/_2H_2(g)$).

Equation 16 can be added to eq 1 to give the more easily interpretable reaction corresponding to the adsorption of OH from the hydroxyl radical in gas phase

$$Pt + OH(g) \rightleftharpoons Pt{-}OH \qquad (17)$$

The values of $\Delta H°$ plotted in Figures 5B and 8B for Pt(111) and Pt(100), respectively, can now be recalculated for reaction 17. Let us focus first on the results for Pt(111). The $\Delta H°$ values found for reaction 3, between 60 and 90 kJ mol^{-1}, give enthalpy changes for reaction 17 ranging between −265 and −235 kJ mol^{-1}. These values can be directly compared with the energies of adsorption calculated by theoretical methods, but taking into account that upon OH adsorption the structure and energetics of the double layer (dl) will change.[14] In principle, this double-layer modification could be taken into account through the following cycle:

$$\begin{array}{ccc} Pt(hkl) & \xrightarrow{+\ solution} & Pt(hkl) - dl \\ \downarrow OH(g) & & OH(g)\downarrow \\ Pt(hkl) - OH & \xrightarrow{+\ solution} & Pt(hkl) - OH - dl' \end{array} \qquad (18)$$

from which we deduce

$$\Delta H°_{ads}(OH_{UPD}) = \Delta H°_{ads}(OH) + \Delta H°_f(dl') - \Delta H°_f(dl) \qquad (19)$$

where $\Delta H°_{ads}(OH_{UPD})$ is the adsorption enthalpy value determined by us for reaction 17, whereas the values calculated theoretically can be taken as good estimates for $\Delta H°_{ads}(OH)$. Finally, the $\Delta H°_f(dl)$ and $\Delta H°_f(dl')$ values correspond to the double layer formation enthalpies for a bare Pt surface and for a Pt surface covered with OH.

A value of −253 kJ mol^{-1} has been obtained for $\Delta H°_{ads}(OH)$ (at low coverage)[34] on the basis of measurements for the kinetics of various surface reactions in gas phase. Several $\Delta H°_{ads}(OH)$ values have been calculated for Pt(111) surfaces. Michaelides and Hu, from density functional theory (DFT) calculations, report values around −220 kJ mol^{-1} for low OH coverage (below 1/3 OH/Pt) and around −240 kJ mol^{-1} for coverages higher than 0.5 OH/Pt.[23] On the other hand, Ishikawa et al. have calculated a value of −221 kJ mol^{-1} for the adsorption energy of OH on a (Pt_3)(Pt_7) cluster.[35] Similar values are found by Karlberg et al. (−222.9 kJ mol^{-1}).[36] A recent paper by Shubina et al. reports a bond energy of OH (on-top site) on Pt(111) of −224.8 kJ mol^{-1}.[37] Let us compare the gas-phase experimental OH adsorption enthalpy value (−253 kJ mol^{-1})[34] with that determined by us for low OH coverage on Pt(111) (−265 kJ mol^{-1}). If one takes into account that the former is subjected to an uncertainty of ±20 kJ mol^{-1}, both values are in very good agreement.

The experimental adsorption enthalpy on Pt(111) electrodes is found to decrease in absolute value with increasing OH coverage. This fact can be rationalized on the basis of the adlayer composition in the different coverage ranges and of the interaction energy of the different hydrogen bonds between adsorbed species. At low coverage, the adsorbing OH forms predominantly OH−water hydrogen bonds, while at high OH coverage, there exists a significant amount of hydrogen bonds between pairs of OH species adsorbed on neighboring sites. Density functional calculations by Karlberg et al.[22] show that on Pt(111) the hydrogen bond between adsorbed water and OH species (37 kJ mol^{-1}) is significantly stronger than the OH_{ads}−OH_{ads} hydrogen bond (19 kJ mol^{-1}). This is in agreement with the coverage behavior of the OH adsorption enthalpy. However,

this is not a complete picture, as other factors, such as the applied external electric field and the interactions with nonchemisorbed species in the double layer, could also play a role.

The values of $\Delta H°$ obtained for reaction 17 on Pt(100) are centered around -280 kJ mol^{-1}. This value is similar to those obtained for Pt(111), indicating that similar bonding energies are involved. As an important difference from the discussion above for Pt(111), on Pt(100) the value of $\Delta H°$ is not very sensitive to coverage. This insensitivity could be related with the square symmetry of the metal surface, which makes the development of an extended structure of hydrogen bonds between the OH and water adsorbed species more difficult. We are not aware of either experimental or calculated values for the adsorption energy of OH on Pt(100).

Parallel to the case of the adsorption enthalpy, the adsorption entropy can be calculated on the basis of experimental results for reaction 3 taking into account reaction 16 to yield finally the value corresponding to reaction 17. The values found for reaction 3 vary in the case of Pt(111) from -20 to 70 J K^{-1} mol^{-1} for increasing coverage values, which once recalculated for eq 17 become -200 (low coverage) and -110 (high coverage) J K^{-1} mol^{-1}, respectively.

To take into account the perturbation produced in the double layer by the adsorption of OH, an equation analogous to eq 19 can be written

$$\Delta S°_{ads}(OH_{UPD}) = \Delta S°_{ads}(OH) + S°_{dl'} - S°_{dl} \qquad (20)$$

where $S°_{dl}$ and $S°_{dl'}$ refer to the absolute standard entropy for the double layer without and with adsorbed OH, respectively, and

$$\Delta S°_{ads}(OH) = S°(OH_{ads}) - S°(OH_g) \qquad (21)$$

The tabulated value[38] of $S°(OH_g)$ at 298 K is 183.74 J K^{-1} mol^{-1}. The absolute entropy of the adsorbed OH species at the solid−gas interphase can be estimated in the mobile and immobile adsorption limiting cases by following the statistical mechanical procedure described in ref 14. The contribution of the vibrational degrees of freedom to the entropy is very low, as $h\nu \gg k_B T$. For our choice of formal standard state for the OH adlayer ($\theta = 0.5$), the configurational contribution to the entropy of the OH adlayer is zero.

The value of $\Delta S°_{ads}(OH_{UPD})$ evaluated for $\theta = 0.5$ at 298 K amounts, for the totally mobile case, to -54.03 J K^{-1} mol^{-1}, and for the immobile case, to close to -182 J K^{-1} mol^{-1}. This latter value lies within the experimental range for $\Delta S°_{ads}(OH_{UPD})$. More concretely, the theoretical value approaches that found in the low coverage range, where the system should behave in a more ideal way. One should note that ideality has been assumed in the evaluation of the absolute entropy of the adsorbed layer.

The adsorption entropy value, together with the bonding strength and with the experimental observation by Bedürftig et al.[21] of frequencies corresponding to hindered translation modes (admittedly at low temperatures), indicates that the adsorption of OH could be considered essentially immobile. However, there is a very significant increase of $\Delta S°_{ads}(OH_{UPD})$ with OH coverage. This would suggest that the OH mobility increases considerably with coverage (provided the absolute entropy double layer values in the absence and in the presence of adsorbed OH are similar). Alternatively, assuming that mobility would not vary with coverage, very important changes in the double-layer entropy due to variations in θ_{OH} should be invoked (see eq 20). From the actual OH data, we cannot decide which of these two limiting scenarios is more plausible. The delocalization of OH could take place, despite the high adsorption energy, via a hydrogen transfer between neighboring OH and water adspecies, probably involving tunneling. This would be in agreement with a recent study of hydroxyl−water coadsorption on Rh(111) that reveals the possibility of an apparent enhanced diffusion of OH on the water-covered metal surface through a Grotthus-like mechanism.[39] Such a strong coverage dependence of the adsorption entropy was not found for H_{UPD}.[14] The H_{ads} species is not integrated in the hydrogen-bonded adlayer network formed by on-top adsorbed water, but lies directly attached to the metal surface, in the threefold hollow sites (much closer to the metal surface plane). In any case, it can be concluded that the competition of water and OH and the ability to form extended mixed structures of adsorbed OH and water linked by hydrogen bonds has an important effect on the thermodynamics of the Pt(111) system.

For Pt(100), $\Delta S°$ values corresponding to reaction 3 are close to zero, giving values for reaction 17 close to -180 J mol^{-1} K^{-1}. This result is consistent with an immobile adlayer, as discussed above for Pt(111). A striking difference between the resulting values of $\Delta S°$ for Pt(111) and Pt(100) is the different dependence with coverage. The small effect of coverage on $\Delta S°$ measured on Pt(100) suggests that the increase of OH coverage does not affect significantly the mobility (diffusion) of the hydroxyl species within the mixed water−OH chemisorbed layer. This is probably a consequence of the mismatch between the square symmetry of the metal surface, and the "hexagonal" of the hydrogen-bonded OH−water structures.

Conclusions

The temperature dependence of the reversible voltammetric adsorption of OH has been studied in 0.1 M perchloric acid, where no significant specific adsorption of anions occurs. A thermodynamic analysis of the overall reaction H_2O + Pt(111) ⇋ Pt(111)−OH + $^1/_2H_2$ has been carried out, yielding values for $\Delta G°$, $\Delta H°$, and $\Delta S°$ for this process, as well as the Frumkin interaction parameter. To facilitate data analysis, from these experimental values, and using the tabulated value for the standard electrode potential corresponding to the formation of water from hydrogen and hydroxyl radical, the corresponding quantities have been obtained for the process: Pt + OH(g) ⇋ Pt−OH.

The adsorption enthalpy for OH on a Pt(111) surface has been estimated to range between -265 and -235 kJ mol^{-1}, in good agreement with the experimental value obtained in gas phase[34] and with theoretical values obtained from density functional theory calculations for this surface.[21,23,36,37] The experimental value obtained for Pt(100), -280 kJ mol^{-1}, is similar to that obtained for Pt(111).

The experimental adsorption entropy for the OH species, despite its strong dependence on OH coverage, agrees well with a localized adsorption of OH on Pt(111), but the strong coverage dependence suggests increased mobility and/or significant changes in double-layer ordering with increasing OH coverage. In the case of Pt(100), adsorption entropy data also agree with an OH immobile adlayer. The absence of a significant variation with coverage in the case of this orientation suggests that an increase of OH coverage does not affect the OH mobility and the surface order in the adlayer. This can be rationalized as a consequence of the square symmetry of the metal topmost layer for this orientation, which makes difficult the development of an extended hydrogen-bonded mixed structure of OH and water adsorbates, thus impeding enhanced surface mobility of the hydroxyl moiety (by H exchange between neighboring adsor-

bates). The interpretation of the entropy values has been done on the basis of similar values for S°_{dl} and $S^{\circ}_{dl'}$. Significant differences between them could explain the dependence of $\Delta S^{\circ}_{ads}(OH_{UPD})$ on θ_{OH} without invoking variation in the mobility of the adsorbate.

We would like to emphasize that electrochemical measurements and a subsequent thermodynamic analysis constitute a convenient procedure for the determination of adsorption energies for species such as OH. As long as the double-layer effects are modest, as seems to be the case from the data presented here and in ref 14, the electrochemically determined values are an accurate alternative to sometimes challenging gas-phase measurements.

In a more general vein, the results reported in this paper and those of ref 14 clearly indicate that the surface structure of the metal substrate plays a central role in determining the structural ordering of the interface, probably through the formation of extended hydrogen-bonded networks, with implications in the thermodynamic behavior of the adsorption/desorption processes on these single-crystal electrodes.

Acknowledgment. This work has been carried out in the framework of projects BQU2003-3737 (Fondos FEDER) and BQU2003-4029 financed by the Ministerio de Ciencia y Tecnología (Spain). V.C. gratefully acknowledges financial support from M.E.C. within the framework of project "Ramón y Cajal".

References and Notes

(1) Feliu, J. M.; Orts, J. M.; Fernández-Vega, A.; Aldaz, A.; Clavilier, J. *J. Electroanal. Chem.* **1990**, *296*, 191.

(2) Markovic, N. M.; Grgur, B. N.; Lucas, C. A.; Ross, P. N. *J. Phys. Chem. B* **1999**, *103*, 487.

(3) Herrero, E.; Alvarez, B.; Feliu, J. M.; Blais, S.; Radovic-Hrapovic, Z.; Jerkiewicz, G. *J. Electroanal. Chem.* **2004**, *567*, 139.

(4) Lebedeva, N. P.; Koper, M. T. M.; Herrero, E.; Feliu, J. M.; van Santen, R. A. *J. Electroanal. Chem.* **2000**, *487*, 37.

(5) Orts, J. M.; Fernández-Vega, A.; Feliu, J. M.; Aldaz, A.; Clavilier, J. *J. Electroanal. Chem.* **1992**, *327*, 261.

(6) Schmidt, T. J.; Ross, P. N.; Markovic, N. M. *J. Phys. Chem. B* **2001**, *105*, 12082.

(7) (a) Breiter, M. W. In *Transactions on the Symposium on Electrode Processes*; Yeager, E., Ed.; John Wiley and Sons: New York, 1961. (b) Breiter, M. *Electrochim. Acta* **1962**, *7*, 25. (c) Breiter, M. W. *Ann. N. Y. Acad. Sci.* **1963**, *101*, 709.

(8) Conway, B. E.; Angerstein-Kozlowska, H.; Sharp, W. B. A. *J. Chem. Soc., Faraday Trans. 1* **1978**, *74*, 1373.

(9) Zolfaghari, A.; Jerkiewicz, G. *J. Electroanal. Chem.* **1997**, *420*, 11.

(10) Zolfaghari, A.; Jerkiewicz, G. *J. Electroanal. Chem.* **1997**, *422*, 1.

(11) Zolfaghari, A.; Jerkiewicz, G. *J. Electroanal. Chem.* **1999**, *467*, 177.

(12) Radovic-Hrapovic, Z.; Jerkiewicz, G. *J. Electroanal. Chem.* **2001**, *499*, 61.

(13) Markovic, N. M.; Schmidt, T. J.; Grgur, B. N.; Gasteiger, H. A.; Behm, R. J.; Ross, P. N. *J. Phys. Chem. B* **1999**, *103*, 8568.

(14) Gómez, R.; Orts, J. M.; Alvarez-Ruiz, B.; Feliu, J. M. *J. Phys. Chem. B* **2004**, *108*, 228.

(15) Michaelides, A.; Ranea, V. A.; De Andrés, P. L.; King, D. A. *Phys. Rev. Lett.* **2003**, *90*, 216102.

(16) Michaelides, A.; Hu, P. *J. Am. Chem. Soc.* **2001**, *123*, 4235.

(17) Wilke, S.; Natoli, V.; Cohen, M. H. *J. Chem. Phys.* **2000**, *112*, 9986.

(18) Vassilev, P.; Louwerse, M. J; Baerends, E. J. *Chem. Phys. Lett.* **2004**, *398*, 212.

(19) Seitsonen, P.; Zhu, Y.; Bedurftig, K.; Over, H. *J. Am. Chem. Soc.* **2001**, *123*, 7347.

(20) Clay, C.; Haq, S.; Hodgson, A. *Phys. Rev. Lett.* **2004**, *92*, 046102.

(21) Bedürftig, K.; Völkening, S.; Wang, Y.; Wintterlin, J.; Jacobi, K.; Ertl, G. *J. Chem. Phys.* **1999**, *111*, 11147.

(22) Karlberg, G. S.; Wahnström, G. *Phys. Rev. Lett.* **2004**, *92*, 136103.

(23) Michaelides, A.; Hu, P. *J. Chem. Phys.* **2001**, *114*, 513.

(24) Clavilier, J. *J. Electroanal. Chem.* **1980**, *107*, 211.

(25) Clavilier, J.; Armand, D.; Sun, S.-G.; Petit, M. *J. Electroanal. Chem.* **1986**, *205*, 267.

(26) Clavilier, J.; El Achi, K.; Petit, M.; Rodes, A.; Zamakhchari, M. A. *J. Electroanal. Chem.* **1990**, *295*, 333.

(27) Blomgren, E.; Bockris, J. O'M. *J. Phys. Chem.* **1959**, *63*, 1475.

(28) Ross, P. N. *Surf. Sci.* **1981**, *102*, 463.

(29) Jerkiewicz, G.; Zolfaghari, A. *J. Phys. Chem.* **1996**, *100*, 8454.

(30) Lasia, A. *J. Electroanal. Chem.* **2004**, *562*, 23.

(31) Conway, B. E.; Angerstein-Kozlowska, H.; Dhar, H. P. *Electrochim. Acta* **1974**, *19*, 455.

(32) The Frumkim adsorption isotherm has been chosen as a reference model behavior in order to carry out the analysis of the experimental results. It should be taken into account that some features of the system studied, such as coadsorption and directional hydrogen bonding, are not explicitly taken into account by the Frumkin isotherm. Besides, as this is a mean-field isotherm, it ignores the spatial structure of the system and cannot describe properly the behavior in the vicinity of phase transitions. The use of Monte Carlo simulation in combination with adequate modeling of the essential physicochemical features of the system for obtaining adsorption isotherms for single-crystal electrodes allows one to overcome these limitations. However, this is out of the scope of this paper. The interested reader can find more information on this topic in the chapter by Brown, G.; Rikvold, P. A.; Mitchell, S. J.; Novotny, M. A. In *Interfacial Electrochemistry. Theory, Experiment, and Applications*; Wieckowski, A., Ed.; M. Dekker: New York, 1999; Chapter 4.

(33) *Standard Potentials in Aqueous Solutions*; Bard, A. J., Parsons, R., Jordan, J., Eds.; M. Dekker: New York, 1985.

(34) Anton, A. B.; Cadogan, D. C. *Surf. Sci. Lett.* **1990**, *239*, L548.

(35) Ishikawa, Y.; Liao, M.-S.; Cabrera, C. R. *Surf. Sci.* **2002**, *513*, 98.

(36) Karlberg, G. S.; Olsson, F. E. Persson, M.; Wahnström, G. *J. Chem. Phys.* **2003**, *119*, 4865.

(37) Shubina, T. E.; Hartnig, C.; Koper, M. T. M. *Phys. Chem. Chem. Phys.* **2004**, *6*, 4215.

(38) *CRC Handbook of Chemistry and Physics*, 74th ed.; Lide, D. R., Ed.; CRC Press: Boca Raton, 1993.

(39) Vassilev, P.; Koper, M. T. M.; van Santen, R. A. *Chem. Phys. Lett.* **2002**, *359*, 337.